

# Ultimate limit of quantum beam tracking

Haoyu Qi,<sup>1,\*</sup> Kamil Brádler,<sup>1</sup> Christian Weedbrook,<sup>1</sup> and Saikat Guha<sup>2</sup>

<sup>1</sup>Xanadu, 372 Richmond St W, Toronto ON, M5V 2L7, Canada

<sup>2</sup>College of Optical Sciences, University of Arizona, 1630 E. University Blvd., Tucson, Arizona 85719, USA

Tracking small transverse displacements of an optical beam with ultra-high accuracy is a fundamental problem underlying numerous important applications ranging from pointing, acquisition and tracking for establishing a lasercom link, to atomic force microscopy for imaging with atomic-scale resolution. Determining what is the optimal quantum-optical probe and the best achievable sensitivity of measuring a small transverse optical beam displacement, is the fundamental question central to these sensing schemes. By mapping this problem to an array of nested Mach-Zehnder interferometers, we explicitly construct the optimal probe state. It is entangled across the spatial modes allowed within the Fresnel number product of the propagation geometry, and entangled across the temporal modes within the time-bandwidth product of the optical probe. We show that the optimal sensitivity of measuring the beam displacement achieves a Heisenberg limited scaling over both the number of temporal modes and the average number of photons transmitted per mode. Surprisingly, we discover a sub-Heisenberg limited scaling over the number of available spatial modes. To qualify the quantum enhancement, we also establish the optimal sensitivity of a classical-light probe, which gives shot-noise limit over both the number of temporal modes and the number of photons per mode, and Heisenberg limited scaling over the number of spatial modes. Finally, we construct an explicit design for quantum-enhanced beam tracking, which uses a Gaussian (multi-mode-entangled squeezed-state) probe and a Gaussian (multi-mode homodyne) receiver.

## I. INTRODUCTION

The precision of optical sensors of both *active* (e.g., laser gyroscopes [1], LIDARs [2], atomic-force microscopes [3], and laser vibrometers [4]), and *passive* (e.g., fluorescence microscopy [5], astronomical imaging [6], and satellite based remote sensing [7]) kinds is often quantified as the standard deviation  $\delta\theta$  of the estimate of desired scene parameter(s)  $\theta$  versus the total mean photon number (a.k.a. power)  $N$  collected over the receiver's integration time. The fundamental precision limit, i.e., the best scaling of  $\delta\theta$  versus  $N$  achievable by using the optimal probe light and the receiver, given the physical constraints of the application scenario, is ultimately governed by quantum mechanics.

When multiple sensors have different *views* of the same scene, pre-shared entanglement across those sensors can improve the attainable precision. This is true both for passive [8] and active [9] sensors. In recent years, several theoretical calculations [10–12] (for active sensing) have indicated that if a set of  $M$  distributed sensors are sensing one aggregate parameter  $\theta$  of the scene, then pre-shared entanglement among the sensors can help improve the sensing precision. As an example, for sensing an average phase modulation across  $M$  sensors, for a total of  $N$  probe photons expended across  $M$  distributed sensors, individual (non-entangled) quantum sensors obtain a standard deviation  $\delta\theta \sim M^{3/2}/N$ . Whereas, a probe entangled across those  $M$  sensors yields  $\delta\theta \sim M/N$  [10]. So, for this problem, shared entanglement improves the sensing precision by a factor of  $\sqrt{M}$ .

One does not need  $M$  physical sensors to see the aforesaid entanglement-assisted performance improvement. As we will show in this paper, entanglement across multiple orthogonal spatio-temporal modes of the probe field—each of which

are non-trivially modulated by the target parameter of interest (and hence can be thought of as “multiple sensors”)—can improve the performance of a standalone active sensor. In particular, we will show such performance improvement in the accuracy of detecting a tiny transverse displacement of a beam over a near-field free-space propagation path (see Fig. 1).

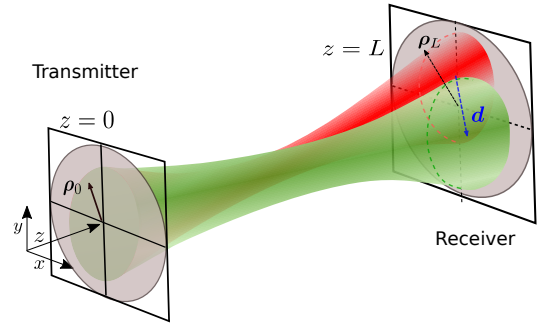


FIG. 1: An  $L$ -meter line-of-sight optical propagation path with circular transmitter and receiver pupils of areas  $A_t$  and  $A_r$ , respectively. We consider the near-field propagation regime, i.e.,  $D \equiv A_t A_r / (\lambda L)^2 \gg 1$ , where  $\lambda$  is the center wavelength of the transmitted light. A transmitter of  $W$  [Hz] optical bandwidth modulates  $M_S \approx D$  near-unity-transmissivity orthogonal spatial modes and  $M_T \approx WT$  orthogonal temporal modes over probing duration  $T$  seconds, with a total of  $N$  mean photon number distributed over  $M = M_S M_T$  modes. The transmitter points the beam towards the center of the receiver aperture. However, there is an unknown transverse (vector) displacement of the beam,  $\mathbf{d}$ , measured in the receiver-aperture plane, whose origin is dependent on the application. The goal of the receiver—via optimal detection of the collected light—is to estimate  $\mathbf{d}$  precisely. In this paper, we will restrict our attention to a scalar beam displacement  $d$  along the  $x$  axis.

\*Electronic address: [haoyu@xanadu.ai](mailto:haoyu@xanadu.ai)

## II. PROBLEM STATEMENT AND BACKGROUND

Accurate estimation of a small transverse displacement of an optical beam is important in many practical applications. Examples include ultra-stable beam pointing, acquisition and tracking for space-based laser communications, in LIDAR receivers, for precision guided munition, ultra-weak absorption measurements, single-molecule tracking [13, 14] in biological imaging and atomic force microscopy, just to name a few. Our goal in this paper is to study the fundamental precision limit of estimating a small transverse displacement  $d$  of an optical beam over a near-field free-space propagation path shown in Fig. 1, and quantify the performance gap between the best classical optical probe and the optimal quantum entangled probe.

The first paper that tackled this problem [15] considered a *split detector*—one which has two pixels separated by an edge—and claimed that no single-mode probe state can surpass the standard quantum limit (SQL) or the so-called *shot noise scaling* of measurement sensitivity. This led the authors to consider multi-spatial-mode probe states, and in particular a two-mode entangled state prepared by interferometrically mixing ideal laser light (coherent state) and squeezed light. They showed that the error of estimating the transverse beam displacement was  $\sim 1/(\sqrt{N}e^r)$ , where  $r$  quantifies the amount of squeezing and  $N$  is the total mean photon number expended during the probing interval. This idea was implemented in a proof-of-concept experiment in [16]. In Ref. [17], this idea, dubbed the “quantum laser pointer”, was generalized to two dimensions and an experiment was carried out.

There were several follow up papers in terms of a more theoretical analysis for this problem. For example, Ref. [18] considered a split detector, used a squeezed light probe, and compared the performance with a photon-number-resolving (PNR) detector array as a baseline. In Ref. [19], the authors calculated the classical Fisher information of the PNR array and that of a split detector, but from an imaging point of view. The quantum Fisher information (QFI) [20, 21] for this problem—a measure of the optimal sensitivity in detecting a parameter embedded in a quantum state with no restrictions imposed on how the quantum state is detected—was considered in Ref. [22]. The problem they considered, that of estimating an arbitrary parameter encoded in a multi-mode Gaussian quantum state, is slightly more general than the problem we consider here, where that parameter is a transverse displacement of a beam. Their conclusion was that the optimal Gaussian state is a coherent state combined with a single-mode squeezed vacuum. However, no statement on Heisenberg limited sensitivity was made, non-Gaussian state probes were not considered, and most importantly, no structured receiver design was proposed or analyzed.

In all of the papers discussed above, the authors assumed a strong coherent state probe, modulated with quadrature-squeezed light. Finding the quantum optimal (potentially spatio-temporal-entangled) probe, its performance, the role of entanglement in space versus time, and structured transmitter-receiver designs to harness this quantum enhancement in the precision of estimating beam displacement were left open.

## III. MAIN RESULTS

Let us consider a quasi-monochromatic  $\lambda$ -center-wavelength source with optical bandwidth  $W$  Hz, in a near-field  $L$ -meter-range line-of-sight propagation geometry shown in Fig. 1, i.e., the Fresnel number product  $D \equiv A_t A_r / (\lambda L)^2 \gg 1$ , where  $A_t$  and  $A_r$  are areas of the transmitter and receiver apertures. There are roughly  $M_S \approx D$  near-unity-transmissivity orthogonal spatial modes and  $M_T \approx WT$  orthogonal temporal modes over a probing duration of  $T$  seconds. The source points the beam towards the center of the receiver aperture. However, there is an unknown transverse displacement of the beam,  $d$ , measured in the receiver-aperture plane, whose origin is dependent on the application. The goal of the receiver—via optimal detection of the collected light—is to estimate  $d$  precisely.

Let us impose a transmit power constraint of  $\bar{n}$  mean photon number per mode, distributed over the  $M = M_S M_T$  spatio-temporal modes. This implies a total of  $N = \bar{n} M_S M_T$  mean photon number over the probing duration, and equivalently a transmit power constraint of  $P = \bar{n} M_S W$  photons per second. Note that power in Watts would be  $P(hc/\lambda)$ , where  $hc/\lambda$  is the photon energy at wavelength  $\lambda$ .

We find the following main results for scaling (constants omitted) of the standard deviation  $\delta d$  of the beam displacement estimate.

1. **Optimal classical probe.** If the transmitted light is constrained to be *classical*, i.e., expressible as a statistical mixture of coherent states of the  $M$  spatio-temporal modes (i.e., have a proper  $P$ -function representation),

$$\delta d \sim \frac{1}{(\sqrt{M_T} M_S \sqrt{\bar{n}})} = \frac{1}{\sqrt{M_S}} \times \frac{1}{\sqrt{PT}}; \quad (1)$$

2. **Optimal spatially-entangled probe.** If we allow the probe to be entangled over all  $M_S$  spatial modes, but there is no entanglement (i.e., product state) across temporal modes, then we have:

$$\delta d \sim \frac{1}{(\sqrt{M_T} M_S^{3/2} \bar{n})} = \frac{W}{\sqrt{M_S}} \times \frac{1}{P\sqrt{T}}; \quad (2)$$

3. **Optimal spatio-temporally entangled probe.** If the optical probe is allowed to be entangled across all  $M_S$  spatial modes and  $M_T$  temporal modes, we have:

$$\delta d \sim \frac{1}{(M_T M_S^{3/2} \bar{n})} = \frac{1}{\sqrt{M_S}} \times \frac{1}{PT}. \quad (3)$$

We expressed  $\delta d$  above in two equivalent forms. The first form shows how  $\delta d$  scales differently with an increasing number of spatial ( $M_S$ ) and temporal ( $M_T$ ) modes, or degrees of freedoms, respectively; as well as with respect to the mean

photon number per mode,  $\bar{n}$ . This mathematical form of scaling is more readily relatable to the existing literature on quantum metrology. One sees that even with a probe entangled over multiple spatial modes (but not across temporal modes), one gets the  $\delta d \sim 1/\bar{n}$  scaling, commonly known as Heisenberg limited (HL) sensitivity, as opposed to  $\delta d \sim 1/\sqrt{\bar{n}}$ , commonly known as the standard quantum limited (SQL) sensitivity of a classical sensor. However, in addition to this Heisenberg limited sensitivity in  $\bar{n}$ , we see how the  $\delta d$  scales in the number of entangled spatial modes ( $1/M_S \rightarrow 1/M_S^{3/2}$ ) and the number of entangled temporal modes ( $1/M_T^{1/2} \rightarrow 1/M_T$ ). In this problem, we see an unconventional quantum improvement in estimation precision with respect to the number of spatial modes. This has to do with a subtlety with regards to how the beam displacement appears as a progressively higher phase modulation in an effective Mach-Zehnder array representation of the modal modulation caused by beam displacement, as the entanglement shifts to higher-order spatial modes (see Fig. 2).

The second form in which we show the scaling of  $\delta d$  for the three cases above is more operational. The number of near-unity-transmissivity spatial modes  $M_S$  is a fixed parameter determined by the channel geometry, so we treat it as a constant. Similarly, the center wavelength  $\lambda$  and the total optical bandwidth around it  $W$  are treated as given. The user controlled parameters are the transmit power  $P$  and the interrogation time  $T$ , where  $PT$  is the total energy. For a classical sensor,  $\delta d \sim 1/\sqrt{PT}$  (SQL), whereas for the optimal spatio-temporally entangled sensor,  $\delta d \sim 1/PT$  (HL). A probe that is only entangled in spatial modes but not in temporal modes achieves an intermediate precision,  $\delta d \sim 1/P\sqrt{T}$ .

In addition to finding the performance of optimal classical and quantum sources, we propose an explicit transceiver design that achieves the optimal quantum scaling of  $\delta d$  using a multi-mode-entangled squeezed-light probe and a multi-mode coherent-detection optical receiver.

#### IV. QUANTUM MODELING OF THE PROBLEM

Consider a line-of-sight free-space diffraction-limited optical transmission setup between two circular-shaped transmitter and receiver apertures with radii  $r_T$  and  $r_R$  respectively, as shown in Fig. 1. An optical source at the transmitter produces a quasi-monochromatic quantum field  $\hat{E}(\mathbf{r}, t)$  of center wavelength  $\lambda$  and optical bandwidth  $W$ , spatially limited to the exit aperture of the transmitter pupil,  $\{\boldsymbol{\rho}_0 : |\boldsymbol{\rho}_0| \leq r_T\}$ , and temporally limited to the interval  $\{t : t_0 - T \leq t \leq t_0\}$ . We use  $\mathbf{r} = (x, y, z)$  for 3D spatial coordinates, and  $\boldsymbol{\rho}_u = (x, y)$  for the transverse spatial coordinates at  $z = u$ . After propagating through  $L$  meters along the  $z$  direction, the field is collected by the entrance pupil of the receiver aperture,  $\{\boldsymbol{\rho}_L : |\boldsymbol{\rho}_L| \leq r_R\}$ . Let us ignore pulse broadening in time due to dispersion. The maximum number of orthogonal temporal modes that can be packed within the probing interval  $T$  is roughly equal to  $M_T = WT$ .

Using the Yuen-Shapiro quantum diffraction theory [23],

the field at the receiver  $\hat{E}_L(\boldsymbol{\rho}_L, t) := \hat{E}(\mathbf{r}, t)|_{z=L}$  is connected to the field at the transmitter  $\hat{E}_0(\boldsymbol{\rho}_0, t) := \hat{E}(\mathbf{r}, t)|_{z=0}$  via the Huygens-Fresnel diffraction integral:  $\hat{E}_L(\boldsymbol{\rho}_L, t) = \int d^2\boldsymbol{\rho}_0 \hat{E}(\boldsymbol{\rho}_0, t - L/c) h(\boldsymbol{\rho}_0 - \boldsymbol{\rho}_L)$ . Here  $h(\boldsymbol{\rho}) = \exp[ikL + ik|\boldsymbol{\rho}|^2/2L]/(i\lambda L)$ , is a linear space-varying impulse response [23], which admits a normal-mode decomposition,  $h(\boldsymbol{\rho}_0 - \boldsymbol{\rho}_L) = \sum_n \sqrt{\eta_n} \Phi_n(\boldsymbol{\rho}_L) \phi_n(\boldsymbol{\rho}_0)$  where  $k = 2\pi/\lambda$  is the wavenumber and  $\{\eta_n\}$  are arranged s.t.  $0 < \eta_0 < \eta_1 < \dots < 1$ . Here  $\{\phi_n(\boldsymbol{\rho}_0)\}$  and  $\{\Phi_n(\boldsymbol{\rho}_L)\}$  are the *normal modes*, complete orthonormal sets of modes at the transmitter and receiver planes, respectively, such that if only the  $\{\phi_n(\boldsymbol{\rho}_0)\}$  mode is modulated at the transmitter aperture, only the  $\{\Phi_n(\boldsymbol{\rho}_L)\}$  mode will be excited at the receiver aperture, but with amplitude attenuation  $\{\eta_n\}$ .

Physically, this decomposition implies that diffraction-limited propagation of a general optical quantum field between two apertures can be thought of as a countably-infinite set of independent lossy bosonic channels:  $\hat{a}_n^{(L)} = \sqrt{\eta_n} \hat{a}_n^{(0)} + \sqrt{1 - \eta_n} \hat{e}_n$ , where  $\hat{\mathbf{a}}_0 := (\hat{a}_0^{(0)}, \hat{a}_1^{(0)}, \dots)$  and  $\hat{\mathbf{a}}^{(L)} := (\hat{a}_0^{(L)}, \hat{a}_1^{(L)}, \dots)$  are the annihilation operators corresponding to the transmitter and receiver pupil normal modes, respectively.  $\{\hat{e}_n\}$  are the annihilation operators of environment modes we must include to preserve commutator brackets. In the near-field regime, i.e., Fresnel number product  $D = (\pi r_T r_R / \lambda L)^2 \gg 1$ , there are roughly  $D$  modes that are essentially lossless, i.e.,  $\eta_n \approx 1$ , for  $0 \leq n < D$  [23].

Now consider a beam displacement  $\mathbf{d} = (d_x, d_y)$  or a rotation  $\theta = |\mathbf{d}|/L$  of the transmitted field. As long as the displacement is small compared to the size of the receiver's aperture, i.e.,  $|\mathbf{d}|/r_R \ll 1$ , these two scenarios can be considered as equivalent. Since the measurement is applied on the received field, we consider the equivalent situation in which the receiver's aperture is displaced by  $-\mathbf{d}$ . Assuming the receiver separates the vacuum-propagation normal modes  $\{\Phi_n(\boldsymbol{\rho}_L)\}$  (since it does not know  $d$  a priori), the multi-spatial-mode input-output relationship is no longer an array of independent beamsplitters. The displacement induces modal cross talk, which can be seen as a spatial-mode transformation,  $\hat{\mathbf{a}}_L \rightarrow U(\mathbf{d}) \hat{\mathbf{a}}_L U(\mathbf{d})^\dagger = \mathbf{S} \hat{\mathbf{a}}_L$ . We can see that the action of displacement is a passive Gaussian unitary transformation [24]. The *coupling matrix*  $\mathbf{S}$  is given by the following overlap integrals between the original and the displaced receiver-pupil normal modes:

$$\mathbf{S}_{mn}(\mathbf{d}) = \int d^2\boldsymbol{\rho}_L \Phi_m^*(\boldsymbol{\rho}_L - \mathbf{d}) \Phi_n(\boldsymbol{\rho}_L). \quad (4)$$

Therefore, the action of the beam displacement on a general multi-spatial-mode quantum state is the unitary  $U(\mathbf{d}) = \exp[-\hat{\mathbf{a}}_L^\dagger (\ln \mathbf{S}(\mathbf{d})) \hat{\mathbf{a}}_L]$ . We should note here that the transformation is unitary since we are assuming the transmitter to be only modulating the lossless modes. If the transmitter modulates more than  $D$  modes, or just one spatial mode in the far field regime ( $D < 1$ ), we must take the losses ( $\eta_n$ ) into account.

Several simplifications are in order. First, in this work we will restrict ourselves to a single-scalar-parameter estimation

problem, by assuming that the direction of displacement (in the  $(x, y)$  plane) is known to the receiver a priori. Without loss of generality, we choose that direction to be the  $x$ -axis, i.e.,  $\mathbf{d} = (d_x, 0)$ . Secondly, in the regime of the displacement being small, i.e.,  $\tilde{d} := d_x/r_R \ll 1$ , we will just keep up to the leading order term in  $\tilde{d}$  in the coupling matrix  $\mathbf{S} = \mathbf{I} - \Gamma\tilde{d} + O(\tilde{d}^2)$ , where,

$$\Gamma_{mn} = r_R \int_{-\infty}^{\infty} dx dy \frac{\partial \phi_m^*(x, y)}{\partial x} \phi_n(x, y). \quad (5)$$

It is evident that  $\Gamma$  is anti-Hermitian, i.e.,  $\Gamma_{mn} = -\Gamma_{nm}^*$ . The unitary in this limit is given by  $U(\tilde{d}) = \exp(i\tilde{d}\hat{H})$ , where

$$\hat{H} = i\hat{a}_L^\dagger \Gamma \hat{a}_L. \quad (6)$$

The Fresnel number product  $D$  separates all normal modes roughly into two sets: lossless and lossy modes. In our 1D problem, fixing the mode index along the  $y$  direction to zero, the number of lossless spatial modes available to us is roughly  $M_S := \sqrt{D}$ . Therefore, we will only modulate the first  $M_S$  modes, since loss is known to be detriment to quantum enhancements in metrology [25]. At first glance, the mode-coupling matrix in Eq. (4) induced by the beam displacement seems to make this truncation impossible. However, intuitively, the spatial mode cross talk should be ‘‘short-ranged’’ (e.g., nearest neighbor in the mode indices) for infinitesimal displacements. As long as we discard all the modes with indices above  $M_S - \kappa$ , where we define the maximal coupling range  $\kappa = \min\{k : \Gamma_{m, m+\kappa+1} = 0\}$ , the leftover subset of modes stays lossless.

For circular hard apertures, the normal modes are the generalized prolate-spheroidal wavefunctions, the analytical form of which are involved [26, 27]. To clearly illustrate the truncation procedure, we will assume Gaussian-attenuation aperture pupils whose normal modes are Hermite-Gaussian (HG) modes [28],  $\Phi_n(x) = \left(\frac{2}{r_R^2}\right)^{\frac{1}{4}} \psi_n\left(\frac{\sqrt{2}x}{r_R}\right)$ . Here  $\psi_n(x) = (2^n n! \sqrt{\pi})^{-\frac{1}{2}} e^{-x^2/2} H_n(x)$  is the Hermite polynomial. We simply ignore the phase factor, since it does not contribute to  $\Gamma$  and our unitary. For HG modes we have  $\kappa = 1$ , that is, only nearest-neighbor couplings exist, as can be seen by directly calculating the coupling matrix [29],

$$\Gamma_{mn} = \sqrt{m}\delta_{m-1, n} - \sqrt{m+1}\delta_{m+1, n}. \quad (7)$$

Therefore, the first  $M_S - 1$  modes comprise a closed lossless subspace under the action of *small* beam displacements.

In summary, our quantum model is fully described by the unitary  $U(\tilde{d}) = \exp[i\tilde{d}\hat{H}]$ , where  $\hat{H} = i\sum_{n=1}^{M_S-1} \sqrt{n} [\hat{a}_n^\dagger \hat{a}_{n-1} - \hat{a}_{n-1}^\dagger \hat{a}_n]$  by using Eq. (7). Hereafter we will not differentiate between the mode operators at the transmitter and those at receiver, since they are the same for the first  $M_S$  modes.

Using the Jordan-Schwinger map [30],  $\hat{J}_x^n = \frac{1}{2}(\hat{a}_{n-1}^\dagger \hat{a}_n + \hat{a}_n^\dagger \hat{a}_{n-1})$ ,  $\hat{J}_y^n = \frac{i}{2}(\hat{a}_n^\dagger \hat{a}_{n-1} - \hat{a}_{n-1}^\dagger \hat{a}_n)$ ,  $\hat{J}_z^n = \frac{1}{2}(\hat{a}_{n-1}^\dagger \hat{a}_{n-1} -$

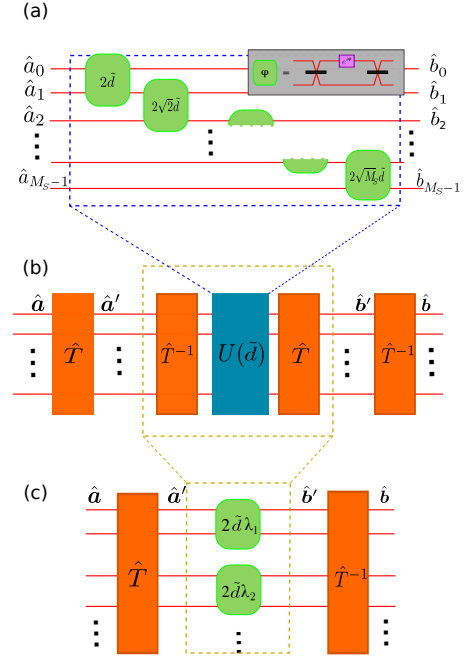


FIG. 2: (a) Unitary quantum model of beam displacement  $\tilde{d}$ . In the limit of  $d = d/r_R \ll 1$  where  $r_R$  is the radius of the receiver aperture, and the near field regime ( $D \gg 1$ ), the effect of beam displacement is a series of pairwise nested Mach-Zehnder interferometer (MZI) interactions on spatial modes  $n$  and  $n-1$ ,  $n = 1, \dots, M_S - 1$ . The  $n$ -th MZI consists of a phase shift of  $2\sqrt{n}\tilde{d}$  sandwiched by two 50-50 beam splitters. (b) By inserting a properly chosen mode transformation  $\hat{T}$  and its inverse on either side of  $U(\tilde{d})$ , we can show that the effective beam displacement unitary  $\hat{T}^{-1}U(\tilde{d})\hat{T}$  in the transformed mode basis is a set of  $M_S/2$  pairwise two-mode MZIs, as shown in (c). The phase of each MZI is given by the eigenvalues of the coupling matrix  $\Gamma$  described in the text, multiplied by  $\tilde{d}$ .

$\hat{a}_n^\dagger \hat{a}_n$ ), the Hamiltonian can be compactly written as follows

$$\hat{H} = \sum_{n=1}^{M_S-1} 2\sqrt{n}\hat{J}_y^n. \quad (8)$$

Each term in the above sum represents a MZI with phase  $2\sqrt{n}\tilde{d}$  [31]. Therefore, in the limit  $\tilde{d} \ll 1$ , the unitary operator  $U(\tilde{d})$  that captures the effect of a small beam displacement factorizes into a form where each mode interacts with its two neighboring modes with a two-mode MZI, as shown in Fig. 2.

In the next three sections, we will quantify the performance of the sensor using the quantum Cramér-Rao bound, which is given by the inverse of QFI. Given  $\nu$  copies of the state  $\rho_d$  (which encodes parameter  $d$ ), it gives a lower bound on the variance of an unbiased estimator constructed from joint quantum measurement at the output, i.e.,

$$\delta d^2 \geq \frac{1}{\nu \mathcal{F}_Q(\rho_d)}. \quad (9)$$

Quantum Cramér-Rao bound is a tighter lower bound compared with that given by the classical Cramér-Rao bound [32] of the outcome of any specific quantum measurement on  $\rho_d$

(see Appendix A). For a unitary of the form  $U = \exp[i\tilde{d}\hat{H}]$ ,  $\tilde{d} = d/r_R$  and a pure input state probe, resulting in an output  $\rho_d$ , the QFI is independent of  $d$  and is simply a constant times the variance  $\Delta^2\hat{H} = \langle\hat{H}^2\rangle - \langle\hat{H}\rangle^2$  of the Hamiltonian  $\hat{H}$ , i.e.,  $\mathcal{F}_Q = (4/r_R^2)\Delta^2\hat{H}$ .

## V. OPTIMUM CLASSICAL PROBE

We first derive the minimum estimation error that could be achieved by a general single-spatial-mode probe state (classical or quantum). Let us consider a probe whose  $j$ th spatial-mode is excited in some state  $|\psi\rangle$  with mean photon number  $N_S$ ,  $j \in [0, M_S - 2]$ , while leaving the other spatial modes in vacuum. The calculation of the variance of the Hamiltonian  $\hat{H}$  is straightforward. The mean value vanishes due to the skew-symmetry of the coupling matrix  $\Gamma$ , i.e.,  $\Gamma^T = -\Gamma$ .  $\langle\hat{H}\rangle = i\langle\Gamma_{00}\hat{a}_0^\dagger\hat{a}_0\rangle = 0$ . For the mean square of  $\hat{H}$ , only the coupling term between the  $j$  and  $j+1$  modes contributes. Therefore, we have  $\Delta^2\hat{H} = N_S\Gamma_{j,j+1}^2 = jN_S$ , which gives  $\mathcal{F}_Q = 4jN_S/r_R^2$ . From Eq. (A2) in Appendix A we know that the minimum error that can be achieved by a single-mode state is  $\delta d = r_R/2\sqrt{jN_S}$ .

Therefore, we conclude that, a single-spatial-mode probe: (1) cannot surpass the SQL, i.e.,  $1/\sqrt{N_S}$  scaling, but (2) populating a higher-order spatial mode (i.e., higher mode index  $j$ ) achieves a better sensitivity.

At first glance, conclusion (1) is rather surprising, considering the fact that the output of the effective multi-mode interferometer in Fig. 2 even if only one of the input modes is excited (e.g., in a squeezed state) with the other inputs in vacuum, is in general an entangled state. But, (1) is consistent with the finding in Ref. [15]. The analysis in [15] leading to their conclusion (that a single-spatial-mode probe cannot beat SQL scaling), however, was restricted to the case of a split-detector receiver. Their result was not conclusive since the most general receiver measurement was not accounted for. Our QFI-based result conclusively rules out the possibility of surpassing SQL scaling with a single-spatial-mode probe, and provides the impetus to consider multi-spatial-mode (and multi-spatio-temporal mode) entangled states.

Our conclusion (2) above, that populating a higher-order mode is able to achieve better accuracy, can be intuitively understood by noticing that a higher-order HG mode oscillates (in space) more rapidly, thereby making it more sensitive to a small transverse spatial shift of the beam. Mathematically, this shows up as the  $\sqrt{j}$  pre-factor in the effective MZI phase accrued in the interference between modes  $j-1$  and  $j$ , as illustrated in Fig. 2. In other words, physically, probing with a high-order spatial mode once is equivalent to probing with a lower-order mode multiple times, since the same beam displacement results in the higher-order mode getting modulated by a larger phase. We should emphasize here that this result is not restricted to HG modes, but is true for any choice of aperture function (and associated normal modes) [29].

Now we are ready to derive the performance of the optimal classical probe. The most general  $M_S - 1$  mode classical state

is a mixture of product of coherent states  $\int d\alpha P(\alpha)|\alpha\rangle\langle\alpha|$ , where  $\alpha := (\alpha_0, \dots, \alpha_{M_S-2})$  and  $P(\alpha)$  is arbitrary probability distribution. As previously mentioned, it is sufficient to consider a pure input state thanks to the convexity of the QFI [33]. So, considering a coherent state  $|\alpha\rangle$  suffices. The next crucial observation is that a coherent state is *always* single (spatio-temporal) mode in an appropriate mode basis [49].

Now invoking our above result for the general single-mode quantum state, the optimal precision is obtained by putting the coherent state in the highest-order normal mode, yielding:

$$\delta d^P \simeq \frac{r_R}{2\sqrt{M_S N_S}} = \frac{r_R}{2M_S\sqrt{\bar{n}}}, \quad (10)$$

where  $\bar{n} = N_S/M_S$  is the mean photon number per mode (ignoring the difference between  $M_S$  and  $M_S - 1$ ).

To generalize the above result to spatio-temporal modes, considering a product of  $M_T$  single-spatial-mode states with precision given in Eq. (10), given the QFI is additive, we have

$$\delta d^P \simeq \frac{r_R}{2\sqrt{M_S M_T N_S}} = \frac{r_R}{2M_S\sqrt{M_T\bar{n}}}. \quad (11)$$

Eq. (11) also follows readily from (10) by replacing  $\bar{n}$  with  $M_T\bar{n}$ ; the rationale being, a coherent state is always single mode, i.e., we can reinterpret the optimal probe as a single spatio-temporal mode coherent state with  $M_T\bar{n}$  mean photons in the highest-order normal mode.

## VI. OPTIMUM ENTANGLED PROBE

We first show that the Hamiltonian in Eq. (8), which describes a set of coupled MZIs, can be transformed into one of a set of independent MZIs (as we will show in Eq. (14)), after a suitable unitary mode-transformation. The problem of finding the optimal multi-mode probe state thereby reduces to finding the optimal probe in a new mode basis, where each mode pair accrues an independent phase (see Fig. 2). Again, we start by focusing on spatial modes, i.e., fixing a particular temporal mode index, and then generalize to the case of using full spatio-temporal modes at the end of this section.

We first insert two pairs of unitaries  $\{\hat{T}, \hat{T}^\dagger\}$  without changing the dynamics, as shown in Fig. 2 (b), i.e.,

$$\hat{a}' := \hat{T}\hat{a}\hat{T}^\dagger \equiv \mathbf{T}\hat{a}, \quad (12)$$

where  $\mathbf{T}$  is the transformation matrix on the annihilation operators induced by the unitary  $\hat{T}$ .

For a skew-symmetric matrix  $\Gamma$  (i.e.,  $\Gamma^T = -\Gamma$ ), there exists an orthogonal transformation  $\mathbf{T}$  [35], such that

$$\mathbf{T}\Gamma\mathbf{T}^T = \bigoplus_{k=1}^{\lceil M_S/2 \rceil} i\sigma_y\lambda_k, \quad (13)$$

where  $\sigma_y = \begin{pmatrix} 0 & -i \\ i & 0 \end{pmatrix}$  is the Pauli Y operator, and  $\{\pm i\lambda_k\}$  are the eigenvalues of the coupling matrix  $\Gamma$  [50]. In general,

finding  $\{\lambda_k\}$  requires solving the roots of the characteristic equation of  $\Gamma$ , for which no analytical formula exists.

We choose  $\hat{T}$  that brings  $\Gamma$  into its aforesaid ‘normal form’ (13). The fact that  $T$  is orthogonal implies that  $\hat{T}$  is a passive Gaussian unitary [24], and hence realizable by a mode transformation.

To re-express the Hamiltonian of Eq. (6) in the new basis  $\hat{a}'$ , we apply Eq. (12) and have  $\hat{H} = i\hat{a}'^\dagger (T\Gamma T^T) \hat{a}'$ . Invoking the transformation in Eq. (13), we have

$$\hat{H} = 2 \sum_{k=1}^{\lceil M_S/2 \rceil} \lambda_k \hat{S}_y^{2k-1}, \quad (14)$$

where  $\hat{S}_y^{2k-1} = \frac{i}{2}(\hat{a}'_{2k-1} \hat{a}'_{2k-2} - \hat{a}'_{2k-2} \hat{a}'_{2k-1})$ . Since each term in the above sum describes an MZI with phase  $2\tilde{d}\lambda_k$  [31], we have re-expressed the action of beam displacement—originally expressed in Eq. (8) as a nearest-neighbor-mode coupled unitary on the  $\hat{a}$  modes—to a pairwise-mode coupled unitary where pairs of  $\hat{a}'$  modes accrue independent MZI phases (See Fig. 2(c)), as described by Eq. (14). For later convenience, we define  $N_k$  to be the average photon number put into the  $k$ th subsystem, i.e., in modes  $2k-1$  and  $2k-2$ .

To construct the  $M_S$ -mode (entangled) state which maximizes the QFI,  $\mathcal{F}_Q = (4/r_R^2)\Delta^2\hat{H}'$ , we first consider an upper bound  $\Delta\hat{H}' \leq \sum_k (s_{\max}^k - s_{\min}^k)/2$  [9], where  $s_{\max}^k (s_{\min}^k)$  is the maximum (minimum) eigenvalue of the  $k$ th two-mode subsystem described by Hamiltonian  $2\lambda_k \hat{S}_y^{2k-1}$ . From the Schwinger representation [37, 38], each subsystem with Hamiltonian  $2\lambda_k \hat{S}_y^{2k-1}$  is equivalent to a spin- $N_k/2$  system, thereby we have  $s_{\max}^k = \lambda_k N_k$  and  $s_{\min}^k = -\lambda_k N_k$ . Summing them together we have  $\Delta^2\hat{H}' \leq (\sum_k \lambda_k N_k)^2$ .

The optimal probe that saturates this upper bound is readily given by the following entangled state in the  $\mathbf{a}'$  basis [9]:

$$|\Psi^E\rangle_{\mathbf{a}'} = \frac{1}{\sqrt{2}} (|+\rangle_{\mathbf{a}'} + |-\rangle_{\mathbf{a}'}), \quad \text{with} \quad (15)$$

$$|+\rangle_{\mathbf{a}'} = \bigotimes_{k=1}^{\lceil M_S/2 \rceil} \hat{R}_x^{2k-1} \left( \frac{\pi}{2} \right) |N_k, 0\rangle_{a'_{2k-1} a'_{2k}}, \quad (16)$$

$$|-\rangle_{\mathbf{a}'} = \bigotimes_{k=1}^{\lceil M_S/2 \rceil} \hat{R}_x^{2k-1} \left( \frac{\pi}{2} \right) |0, N_k\rangle_{a'_{2k-1} a'_{2k}}. \quad (17)$$

The states  $|\pm\rangle_{\mathbf{a}'}$  correspond to putting all the spins into up (resp., down) along the  $y$  direction. The optimal probe in the original  $\hat{a}$  mode basis is readily obtained by applying the  $M_S$ -mode linear transformation  $\hat{T}^\dagger$  on  $|\Psi^E\rangle_{\mathbf{a}'}$ .

For a given photon-number distribution across spatial modes  $\{N_k\}$ , the optimal QFI achieved by this entangled probe is given by  $4(\sum_k \lambda_k N_k)^2/r_R^2$ . However, we can further optimize the QFI over all possible photon number distributions. Define ratio  $c_k = N_k/N_S$  such that  $\sum_{k=1}^{\lceil M_S/2 \rceil} c_k = 1$ . The QFI given by  $4(\sum_k \lambda_k N_k)^2/r_R^2 = 4N_S^2(\sum_k \lambda_k c_k)^2/r_R^2$  is maximized by choosing  $c_k = \lambda_k/\sum_k \lambda_k$ . Finally, we have the optimal QFI achieved by this choice of photon distribu-

tion,

$$\mathcal{F}_Q^E = \frac{4N_S^2}{r_R^2} \left( \frac{\sum_k \lambda_k^2}{\sum_k \lambda_k} \right)^2. \quad (18)$$

To study the asymptotical behavior of the QFI, notice that  $\sum_k \lambda_k^p = \frac{1}{2}\|\Gamma\|_p^p$ , where  $\|\Gamma\|_p$  is the Schatten  $p$ -norm of  $\Gamma$ . In the limit of  $M_S \gg 1$  we have  $\|\Gamma\|_2 \simeq M_S$  and  $\|\Gamma\|_1 \simeq M_S^{3/2}$  [29]. Therefore, we have following minimum estimation error,

$$\delta d^E \simeq \frac{r_R}{\sqrt{M_S N_S}}. \quad (19)$$

This sub-Heisenberg scaling behavior is actually a composite effect of the spatial entanglement of the probe [9] and the phase gradient in our Hamiltonian  $\hat{H}$  in (14) [39], i.e., increasing  $\lambda_k$  values in the effective MZI array in Fig. 2(c). The former contributes to the HL scaling while the latter leads to another  $\sqrt{M_S}$  enhancement in the sensitivity.

So far we have been considering spatial modes. Our results can be readily generalized to include the use of all temporal modes available. If we don't entangle across the temporal mode index, i.e., consider a product state over the  $M_T$  orthogonal temporal modes, we have the following precision for this hybrid probe (entangled in space but not over time), we get

$$\delta d^H \simeq \frac{d_R}{\sqrt{M_T M_S^{3/2} \bar{n}}}, \quad (20)$$

from the additivity of the QFI.

On the other hand, the optimal spatio-temporal probe state is an entangled state across *both* the spatial and the temporal indexes. For  $M_T$  temporal-modes, effectively we have  $M_T$  copies of the original coupling matrix,  $\bigoplus_{i=1}^{M_T} \Gamma$ . Therefore, by simply redefining  $c_k = \lambda_k/\sum_{k=1}^{M_S M_T/2} \lambda_k$ , we get an optimal QFI with the same form as in Eq. (18), with  $N_S$  replaced by  $N$ . It is not difficult to see that the terms inside of the bracket in Eq. (18) stay the same, thanks to the periodicity of  $\{\lambda_k\}$ . Therefore, the best precision obtained by using a probe entangled across all the spatio-temporal modes is given by

$$\delta d^E \simeq \frac{r_R}{\sqrt{M_S N}} = \frac{r_R}{M_T M_S^{3/2} \bar{n}}. \quad (21)$$

## VII. STRUCTURED MULTI-MODE SQUEEZED-LIGHT TRANSCEIVER ARCHITECTURE

Although we found the optimal spatio-temporally-entangled quantum probe in section VI, designing an explicit transmitter and receiver design for that probe is difficult. In this section, we construct a fully structured transceiver design that involves a Gaussian (multi spatio-temporally-entangled squeezed-state) probe and a Gaussian (homodyne-like) measurement, which attains the quantum-optimal scaling with respect to  $M_T$ ,  $M_S$  and  $\bar{n}$ , as in Eq. (21). We again first consider the  $M_T = 1$  case, since generalization to  $M_T > 1$  is straightforward.



In this case, the block-diagonalized unitary is given by repeating the MZI-array shown in Fig. 3  $M_T$  times. The energy distributions for the coherent states stay the same for each temporal mode index, i.e.,  $c_k = \lambda_k / \sum_{k=1}^{M_S M_T/2} \lambda_k$ . Therefore, the estimator in Eq. (22) remains the same, with the upper limit of summation being extended from  $M_S/2$  to  $M_T M_S/2$  and  $N_S$  being replaced by  $N$ . Same as when we considered non-Gaussian optimal states,  $A$  is invariant under this extension for the eigenvalues  $\{\lambda_k\}$  are periodic. At last, we just need a  $M_T M_S/2$  mode beamsplitter array, such that  $\hat{a}'_0 = \sum_k \sqrt{c_k} \hat{\gamma}_k^s$ , to entangle across all spatial-temporal modes. Putting a squeezed vacuum in mode  $\hat{a}'_0$  with average photon number  $N_s = N/2$ , we get the same minimum estimation error as in Eq. (21).

Finally, let us discuss how one might assemble a transceiver structure for the entangled Gaussian transmitter developed in this section. A notional schematic is shown in Fig. 4. The transmitter generates multi-spatial-mode squeezed light using an optical parameter amplifier (OPA) with a known modal squeezing content [40], which is then transformed into the desired spatially-entangled squeezed state using a universal volumetric mode sorter. Many physical realizations of spatial mode-transformation devices have been explored in the literature. One of those, which uses a stratified free-space propagation through an isotropic medium interspersed with phase masks (which can be realized for example with spatial light modulators or deformable mirrors) [41] can in principle realize arbitrary multi-spatial-mode transformations [42]. The multimode quadrature displacement caused due to the injected coherent states shown in Fig. 3 is realized by mixing the multi-mode entangled squeezed light with an appropriately phase-and-amplitude modulated high-intensity local oscillator laser on a highly-transmissive (e.g., 99:1) beam splitter [43]. At the receiver, we need another volumetric spatial mode transformation followed by a succession of mode-selective homodyne detections, which can in turn be implemented using a quantum-state-preserving mode-selective frequency up-conversion of one mode at a time using non-linear sum-frequency generation (SFG) [44]. The generalization of this architecture to spatio-temporal entanglement follows in a straightforward way. The entire architecture can in principle be realized with available technology.

## VIII. DISCUSSION AND CONCLUSION

We establish the ultimate quantum limit of the accuracy with which one can detect a small lateral movement of an optical beam. We explicitly construct the optimal entangled probe and discover a sub-Heisenberg-limit scaling over the number of spatial modes. We also prescribe a multi-mode Gaussian probe and receiver construct which achieves the quantum optimal precision. Since the production, transformation and detection of Gaussian quantum states (multi-mode squeezed

states) is much less demanding than those of non-Gaussian states, this scheme is far more feasible to realize in the near term compared to other applications of photonic quantum enhancements, such as universal photonic quantum computing or all-optical repeaters for entanglement distribution.

In biological applications, it is important to get a high quality image while ensuring the cellular processes being investigated are in their *in vitro* state [45], which imposes a significant constraint on the probe illumination power. Since our scheme can obtain a desired accuracy with far less illumination power compared with a classical probe, and since spatial-entanglement enhancement is possible only in the diffraction-limited near-field regime, our results are particularly important for biological imaging applications such as molecular tracking or cellular imaging [13, 14]. The low probe power also makes this scheme attractive for covert sensing [46] where the goal of the sensor is to prevent the detection of the optical probing attempt by an adversary by hiding the probe signal within the thermal noise floor.

Our analysis in this paper ignored any loss in propagation, light generation or detection. Even though diffraction-limited propagation loss is essentially negligible in the near-field regime, loss contribution from scattering and absorption in propagation, as well as losses within the source and receiver (e.g., from sub-unity-efficiency detection and mode transformation losses) is inevitable. For other applications of ultra-sensitive beam displacement estimation, such as pointing and acquisition for a far-field lasercom link, diffraction-limited loss must be taken into account. While we leave the analysis of the effect of loss on the sensitivity to a separate future investigation, recent related work [12] suggests that the effect of loss can be alleviated by increasing the number of modes while keeping the total average photon number fixed.

Even though our analysis in this paper was for a one-dimensional setting, generalizing to two dimensional (i.e., vector) displacements is straightforward. One interesting direction of future work would be to generalize our results on estimation of a (given, constant) beam displacement to the precision of tracking of a (temporally-varying) beam displacement. Another intriguing future direction is to study quantum enhancements in sensing both transverse and longitudinal movement of an optical beam, with applications to vibrometry, doppler ranging, and 3D imaging. We conjecture that in such scenarios, the optimal probe could achieve sub-Heisenberg-limit scaling over both the number of spatial modes and the number of temporal modes.

## Acknowledgments

SG would like to thank Zheshen Zhang for introducing him to the results in [12], and Linran Fan for helpful comments on the manuscript. HQ is grateful to Zachary Vernon, Casey Myers, Krishna Sabapathy and Daiqin Su for helpful discussions.

[1] B. Lee, *Optical fiber technology* **9**, 57 (2003).

[2] M.-C. Amann, T. M. Bosch, M. Lescure, R. A. Myllylae, and

- M. Rioux, *Optical engineering* **40**, 10 (2001).
- [3] P. Eaton and P. West, *Atomic force microscopy* (Oxford University Press, 2010).
- [4] P. Castellini, M. Martarelli, and E. Tomasini, *Mechanical Systems and Signal Processing* **20**, 1265 (2006).
- [5] J. W. Lichtman and J.-A. Conchello, *Nature methods* **2**, 910 (2005).
- [6] S. B. Howell, *Handbook of CCD astronomy*, Vol. 5 (Cambridge University Press, 2006).
- [7] J. J. Degnan, *Contributions of space geodesy to geodynamics: technology* **25**, 133 (1993).
- [8] D. Gottesman, T. Jennewein, and S. Croke, *Physical Review Letters* **109**, 070503 (2012).
- [9] V. Giovannetti, S. Lloyd, and L. Maccone, *Physical Review Letters* **96**, 010401 (2006).
- [10] P. C. Humphreys, M. Barbieri, A. Datta, and I. A. Walmsley, *Physical Review Letters* **111**, 070403 (2013).
- [11] T. J. Proctor, P. A. Knott, and J. A. Dunningham, *Physical Review Letters* **120**, 080501 (2018).
- [12] Q. Zhuang, Z. Zhang, and J. H. Shapiro, *Physical Review A* **97**, 032329 (2018).
- [13] M. A. Taylor, J. Janousek, V. Daria, J. Knittel, B. Hage, H.-A. Bachor, and W. P. Bowen, *Nature Photonics* **7**, 229 (2013).
- [14] M. A. Taylor, J. Janousek, V. Daria, J. Knittel, B. Hage, H.-A. Bachor, and W. P. Bowen, *Physical Review X* **4**, 011017 (2014).
- [15] C. Fabre, J.-B. Fouet, and A. Matre, *Optics Letters* **25**, 76 (2000).
- [16] N. Treps, U. Andersen, B. Buchler, P. K. Lam, A. Maitre, H.-A. Bachor, and C. Fabre, *Physical Review Letters* **88**, 203601 (2002).
- [17] N. Treps, N. Grosse, W. P. Bowen, C. Fabre, H.-A. Bachor, and P. K. Lam, *Science* **301**, 940 (2003).
- [18] M. T. L. Hsu, V. Delaubert, P. K. Lam, and W. P. Bowen, *Journal of Optics B: Quantum and Semiclassical Optics* **6**, 495 (2004).
- [19] V. Delaubert, N. Treps, C. Fabre, H. A. Bachor, and P. Réfrégier, *EPL (Europhysics Letters)* **81**, 44001 (2008).
- [20] S. L. Braunstein and C. M. Caves, *Physical Review Letters* **72**, 3439 (1994).
- [21] S. L. Braunstein, C. M. Caves, and G. J. Milburn, *Annals of Physics* **247**, 135 (1996).
- [22] O. Pinel, J. Fade, D. Braun, P. Jian, N. Treps, and C. Fabre, *Physical Review A* **85**, 010101 (2012).
- [23] H. Yuen and J. Shapiro, *IEEE Transactions on Information Theory* **24**, 657 (1978).
- [24] C. Weedbrook, S. Pirandola, R. García-Patrón, N. J. Cerf, T. C. Ralph, J. H. Shapiro, and S. Lloyd, *Reviews of Modern Physics* **84**, 621 (2012).
- [25] R. Demkowicz-Dobrzański, J. Kołodyński, and M. Guţă, *Nature Communications* **3**, 1063 (2012).
- [26] D. Slepian, *Bell Labs Technical Journal* **43**, 3009 (1964).
- [27] D. Slepian, *JOSA* **55**, 1110 (1965).
- [28] J. Shapiro, S. Guha, and B. Erkmen, *Journal of Optical Networking* **4**, 501 (2005).
- [29] See supplementary materials for detailed calculations or proofs.
- [30] J. J. Sakurai and E. D. Commins, *Modern quantum mechanics, revised edition* (AAPT, 1995).
- [31] R. Demkowicz-Dobrzański, M. Jarzyna, and J. Kołodyński, in *Progress in Optics*, Vol. 60 (Elsevier, 2015) pp. 345–435.
- [32] S. K. Sengupta, *Fundamentals of statistical signal processing: Estimation theory* (Taylor & Francis Group, 1995).
- [33] A. Fujiwara, in *Asymptotic theory of quantum statistical inference: selected papers* (World Scientific, 2005) pp. 487–493.
- [34] In order to see why, we observe that a linear-optical unitary acting on a product coherent state (expressed in some orthonormal mode basis),  $|\alpha\rangle$  produces another product coherent state (in that same mode basis)  $|\beta\rangle$  with  $\beta = U\alpha$ , with  $U$  a complex-valued unitary matrix. Therefore the coherent state  $|\alpha\rangle$  can always be thought of as a single-mode coherent state in an appropriate mode basis, and thus a unit vector in an orthonormal set constructed via a Gram-Schmidt orthogonalization where rest of the modes are in their vacuum states.
- [35] H. W. Eves, *Elementary matrix theory* (Courier Corporation, 1966).
- [36] For  $M_S$  odd, the last row and column of the transformed  $\Gamma$  matrix are zeros and thus can be dropped. Therefore, we can take  $M_S$  to be even without loss of generality.
- [37] J. Schwinger, *Quantum theory of angular momentum*, L. Biedenharn and H. Van Dam, eds (Academic Press, New York, 1965).
- [38] B. Yurke, S. L. McCall, and J. R. Klauder, *Physical Review A* **33**, 4033 (1986).
- [39] G. M. D’Ariano and M. G. Paris, *Physical Review A* **55**, 2267 (1997).
- [40] Y. B. Kwon, M. Giribabu, C. Langrock, M. M. Fejer, and M. Vasilyev, in *CLEO: QELS Fundamental Science* (Optical Society of America, 2017) pp. FF2E–2.
- [41] J.-F. Morizur, L. Nicholls, P. Jian, S. Armstrong, N. Treps, B. Hage, M. Hsu, W. Bowen, J. Janousek, and H.-A. Bachor, *JOSA A* **27**, 2524 (2010).
- [42] Z. Borevich, *Journal of Soviet Mathematics* **17**, 1718 (1981).
- [43] M. G. Paris, *Physics Letters A* **217**, 78 (1996).
- [44] P. Manurkar, N. Jain, M. Silver, Y.-P. Huang, C. Langrock, M. M. Fejer, P. Kumar, and G. S. Kanter, *Optica* **3**, 1300 (2016).
- [45] R. Cole, *Cell adhesion & migration* **8**, 452 (2014).
- [46] B. A. Bash, C. N. Gagatsos, A. Datta, and S. Guha, in *Information Theory (ISIT), 2017 IEEE International Symposium on* (IEEE, 2017) pp. 3210–3214.
- [47] According to the Schimdt decomposition, any mixed state can be decomposed into a mixture of pure states:  $\rho = \sum_x p(x)|x\rangle\langle x|$ . The output state is thus given by  $\rho(\theta) = \sum_x p(x)U(\theta)|x\rangle\langle x|U^\dagger(\theta)$ . Applying the concavity of QFI, we have  $\max_\rho \mathcal{F}_Q(\rho) \leq \max_x \mathcal{F}_Q(U(\theta)|x\rangle)$ .
- [48] D. Dominici, *Journal of Difference Equations and Applications* **13**, 1115 (2007).
- [49] In order to see why, we observe that a linear-optical unitary acting on a product coherent state (expressed in some orthonormal mode basis),  $|\alpha\rangle$  produces another product coherent state (in that same mode basis)  $|\beta\rangle$  with  $\beta = U\alpha$ , with  $U$  a complex-valued unitary matrix. Therefore the coherent state  $|\alpha\rangle$  can always be thought of as a single-mode coherent state in an appropriate mode basis, and thus a unit vector in an orthonormal set constructed via a Gram-Schmidt orthogonalization where rest of the modes are in their vacuum states.
- [50] For  $M_S$  odd, the last row and column of the transformed  $\Gamma$  matrix are zeros and thus can be dropped. Therefore, we can take  $M_S$  to be even without loss of generality.

## Supplementary Materials

### Appendix A: Classical and quantum Fisher information

Consider the problem of estimating a parameter  $d$  encoded in a quantum state  $\rho_d$  by making a suitable joint measurement on  $\nu$  independent copies of  $\rho_d$ . A quantum measurement on one copy of  $\rho_d$ , described by positive-operator valued measurement  $\{\Lambda_m\}$ , produces a measurement outcome  $m$  with probability distribution  $p(m; d) = \text{Tr}\{\rho_d \Lambda_m\}$ . Assuming the same measurement is performed on all  $\nu$  copies of  $\rho_d$ , the minimum error of estimating  $d$  (from  $\nu$  i.i.d. samples of  $m$  drawn from the distribution  $p(m; d)$ ) using an unbiased estimator is lower bounded by the inverse of the *classical Fisher information* (CFI),  $\mathcal{F}_C(p) = \int dm p(m; d) \frac{\partial^2}{\partial d^2} \ln p(m; d)$ , also known as the *Cramér-Rao bound*. In other words,

$$\delta d^2 \geq \frac{1}{\nu \mathcal{F}_C(\rho_d, \{\Lambda_m\})}, \quad (\text{A1})$$

If we optimize this classical Cramer-Rao bound over all possible measurement choices, the ultimate error of any unbiased estimator of the displacement  $d$ , is given by the *quantum Cramér-Rao bound* [20, 21], which in general gives a tighter bound compared to classical Cramér-Rao bound corresponding to any specific measurement  $\{\Lambda_m\}$ :

$$\delta d^2 \geq \frac{1}{\nu \mathcal{F}_Q(\rho_d)} \geq \frac{1}{\nu \mathcal{F}_C(\rho_d, \{\Lambda_m\})}, \quad \forall \{\Lambda_m\}. \quad (\text{A2})$$

Here,  $\mathcal{F}_Q$  is called the *quantum Fisher information* (QFI), which is a function just of  $\rho_d$ , i.e., calculating the QFI does not require us to specify a measurement. Specifically, the QFI is given by the following expectation value,

$$\mathcal{F}_Q(\rho_d) = \text{Tr}\{\rho_d L(\rho_d)^2\}, \quad (\text{A3})$$

where the Hermitian operator  $L(\rho_d)$  is the so-called *symmetric logarithm derivative operators* (SLD). When written in the eigenbasis of state  $\rho_d = \sum_i \lambda_i(d) |\lambda_i(d)\rangle \langle \lambda_i(d)|$ , the SLD explicitly reads:

$$L(\rho_d) = \sum_{i,j} \frac{2\langle \lambda_i(d) | \dot{\rho}_d | \lambda_j(d) \rangle}{\lambda_i(d) + \lambda_j(d)} |\lambda_i(d)\rangle \langle \lambda_j(d)|, \quad (\text{A4})$$

where the sum takes over all non-vanishing eigenvalues. Just like CFI, the QFI defined above is also additive, i.e.,  $\mathcal{F}_Q(\rho_d^{\otimes N}) = N \mathcal{F}_Q(\rho_d)$ . It was further shown that the quantum Cramér-Rao bound can always be saturated asymptotically by maximum likelihood estimation and a projective measurement in the eigenbasis of the SLD [20, 21].

A particular useful and relevant formalism for us is the QFI of the output state resulting from a unitary evolution of a pure input state,  $|\psi_d\rangle = e^{i\hat{H}d} |\psi\rangle_{\text{in}}$ . In this case, Eq. (A3) reduces to

$$\mathcal{F}_Q(|\psi_d\rangle) = 4 \left[ \langle \psi_d | \hat{H}^2 | \psi_d \rangle - \left| \langle \psi_d | \hat{H} | \psi_d \rangle \right|^2 \right]. \quad (\text{A5})$$

For the problem being considered in this paper, we are aiming at finding the optimal input (probe) state that results in a modulated state  $\rho_d$  with the highest QFI. Therefore, it suffices for us to just consider pure input states, thanks to the convexity of QFI [33][?]. For a unitary of the form  $\exp[i\tilde{d}\hat{H}]$ ,  $\tilde{d} = d/r_R$  and a pure input state, the QFI is independent of  $d$  and is given by following quantity, proportional to the variance of the Hamiltonian  $\hat{H}$ :  $\mathcal{F}_Q = \frac{4}{r_R^2} \left( \langle \hat{H}^2 \rangle - \langle \hat{H} \rangle^2 \right)$ .

### Appendix B: Hermite-Gaussian modes

In this section we review and derive some basis properties of Hermite-Gaussian modes. We first define *Hermite function* of order  $n$ :

$$\psi_n(x) = (2^n n! \sqrt{\pi})^{-\frac{1}{2}} e^{-x^2/2} H_n(x). \quad (\text{B1})$$

Then the Hermite-Gaussian modes with waist size  $w_0$  are given by

$$u_n(x) = \left( \frac{2}{w_0^2} \right)^{\frac{1}{4}} \psi_n \left( \frac{\sqrt{2}x}{w_0} \right). \quad (\text{B2})$$

The matrix  $\Gamma_{mn}$  is central to our calculation, which is given by

$$\Gamma_{mn} = \int_{-\infty}^{\infty} dx u'_m(x) u_n(x), \quad (\text{B3})$$

$$= \frac{\sqrt{2}}{w_0} \int_{-\infty}^{\infty} dx \psi'_m(x) \psi_n(x), \quad (\text{B4})$$

$$= \frac{\sqrt{2}}{w_0} \int_{-\infty}^{\infty} dx \left[ \sqrt{\frac{m}{2}} \psi_{m-1}(x) - \sqrt{\frac{m+1}{2}} \psi_{m+1}(x) \right] \psi_n(x), \quad (\text{B5})$$

$$= \frac{1}{w_0} [\sqrt{m} \delta_{m-1,n} - \sqrt{m+1} \delta_{m+1,n}]. \quad (\text{B6})$$

Therefore, only nearest-neighbour coupling exists.

### Appendix C: Single-mode probe cannot beat SQL

Here we consider an arbitrary choice of orthonormal modes  $\{u_n(x)\}$  with annihilation operators  $\{\hat{a}_n\}$ . Without loss of generality, consider a single-mode state on the zero mode as follows,

$$|\psi\rangle \otimes |0 \dots 0 \dots\rangle. \quad (\text{C1})$$

The calculation of the variance  $\Delta^2 \hat{H}$  is straightforward. For the expectation value we have

$$\langle \hat{H} \rangle = -i \sum_{mn} \langle \Gamma_{mn} \hat{a}_m^\dagger \hat{a}_n \rangle \quad (\text{C2})$$

$$= -i \Gamma_{00} \langle \psi | \hat{a}_0^\dagger \hat{a}_0 | \psi \rangle = 0. \quad (\text{C3})$$

We thus have  $\Delta^2 \hat{H} = \langle \hat{H}^2 \rangle$ , which is equal to

$$\langle \hat{H}^2 \rangle = - \sum_{mn} \sum_{kl} \Gamma_{mn} \Gamma_{kl} \langle \hat{a}_m^\dagger \hat{a}_n \hat{a}_k^\dagger \hat{a}_l \rangle \quad (\text{C4})$$

$$= - \sum_{n,k} \Gamma_{0n} \Gamma_{k0} \langle \hat{a}_0^\dagger \hat{a}_n \hat{a}_k^\dagger \hat{a}_0 \rangle \quad (\text{C5})$$

$$= - \sum_{n=0}^{\infty} \Gamma_{0n} \Gamma_{n0} \langle \psi | \hat{a}_0^\dagger \hat{a}_0 | \psi \rangle \quad (\text{C6})$$

$$= \Gamma_{0n} \Gamma_{0n}^* N_S. \quad (\text{C7})$$

Using the completeness relation  $\sum_n u_n(x) u_n^*(x') = \delta(x - x')$ , we have

$$\delta d = \frac{C}{2\sqrt{N}} \quad (\text{C8})$$

where

$$1/C^2 = \int dx \left| \frac{\partial u_0(x)}{\partial x} \right|^2. \quad (\text{C9})$$

Therefore, we have prove that single-mode state cannot beat SQL for any choice of orthonormal modes, and higher-order spatial modes gives better sensitivity.

### Appendix D: Asymptotic behaviour of the Schatten norm of the coupling matrix

As shown above, coupling matrix for HG modes is given by the following skew-symmetric matrix

$$\mathbf{\Gamma}(M) = \begin{bmatrix} 0 & 1 & 0 & \dots & 0 \\ -1 & 0 & \sqrt{2} & \dots & 0 \\ 0 & -\sqrt{2} & 0 & \ddots & \vdots \\ \vdots & \vdots & \ddots & \ddots & \sqrt{M-1} \\ 0 & 0 & \dots & -\sqrt{M-1} & 0 \end{bmatrix}, \quad (\text{D1})$$

The eigenvalues of any skew-symmetric matrix are imaginary pairs  $\{\pm i\lambda_k\}$  where  $\lambda_k > 0$ . Therefore the sum of power of  $\lambda_k$  is related to the schatten norm

$$\sum_i \lambda_i^p = \frac{1}{2} |\mathbf{\Gamma}|_p^p. \quad (\text{D2})$$

From the main text, to calculate the QFI of optimum entangled probe we need to know the sum for  $p = 2$  and  $p = 1$  in the limit  $M \gg 1$ . The former is straightforward to calculate :

$$\sum_k \lambda_k^2 = -\frac{1}{2} \text{Tr} \{ \mathbf{\Gamma}^2 \} \quad (\text{D3})$$

$$= -\frac{1}{2} \sum_{nm} \mathbf{\Gamma}_{mn} \mathbf{\Gamma}_{nm} \quad (\text{D4})$$

$$= \frac{1}{2} \sum_{n=1}^{M-1} n = \frac{M(M-1)}{4}, \quad (\text{D5})$$

where we use  $\mathbf{\Gamma}_{mn}$  for HG modes in Eq. (7).

The calculation when  $p = 1$  is more complicated. We first observe that the symmetric version of  $\mathbf{\Gamma}$

$$\tilde{\mathbf{\Gamma}}(M) = \begin{bmatrix} 0 & 1 & 0 & \dots & 0 \\ 1 & 0 & \sqrt{2} & \dots & 0 \\ 0 & \sqrt{2} & 0 & \ddots & \vdots \\ \vdots & \vdots & \ddots & \ddots & \sqrt{M-1} \\ 0 & 0 & \dots & \sqrt{M-1} & 0 \end{bmatrix}, \quad (\text{D6})$$

has eigenvalues  $\{\pm \lambda_i\}$ . Thus, for our purpose it is sufficient to consider the symmetric matrix above. Next, we observe that the characteristic polynomial of  $\tilde{\mathbf{\Gamma}}$  is proportional to the Hermite polynomial,  $2^{-M/2} H_M(\lambda/\sqrt{2})$ . Arranging  $\{\lambda_k\}$  such that they are decreasing, the asymptotic form of  $\lambda_k$  is given by [48]

$$\begin{cases} \lambda_k \simeq \sqrt{M} + O(M^{1/6}), & \text{for } k = O(1), \\ \lambda_k \simeq \frac{\pi}{4}(M - 2k) [M^{-1/2} + O(M^{-3/2})], & \text{for } k = O(n/2). \end{cases} \quad (\text{D7})$$

From which we can see that  $\sum_k \lambda_k \simeq M^{3/2}$ .